Electronic Supplementary Material (ESI) for Journal of Materials Chemistry C.

Supporting information

A Thermally Stable and Reversible Microporous Hydrogen-Bonded Organic Framework: Aggregation Induced Emission and Metal Ion-sensing Properties

Hui Zhou,[a] Qun Ye,[a] Xiangyang Wu,[b] Jing Song,[a] Ching Mui Cho,[a] Yun Zong,[a] Ben Zhong Tang,*[c] T. S. Andy Hor,[ad] Edwin Kok Lee Yeow,[b] and Jianwei Xu*[ad]

*Corresponding author: Jianwei Xu
Email address: jw-xu@imre.a-star.edu.sg

Mailing address: 3 Research Link, Singapore 117602

Tel: 65-6872-7543

Fax: 65-6872-7528

Table content

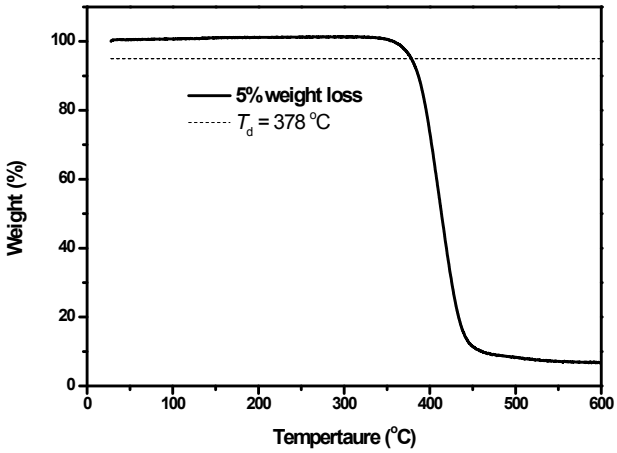

Fig. S1 TGA thermogram of POSS-T_8B recorded at a heating rate of 20 °C/min in air.

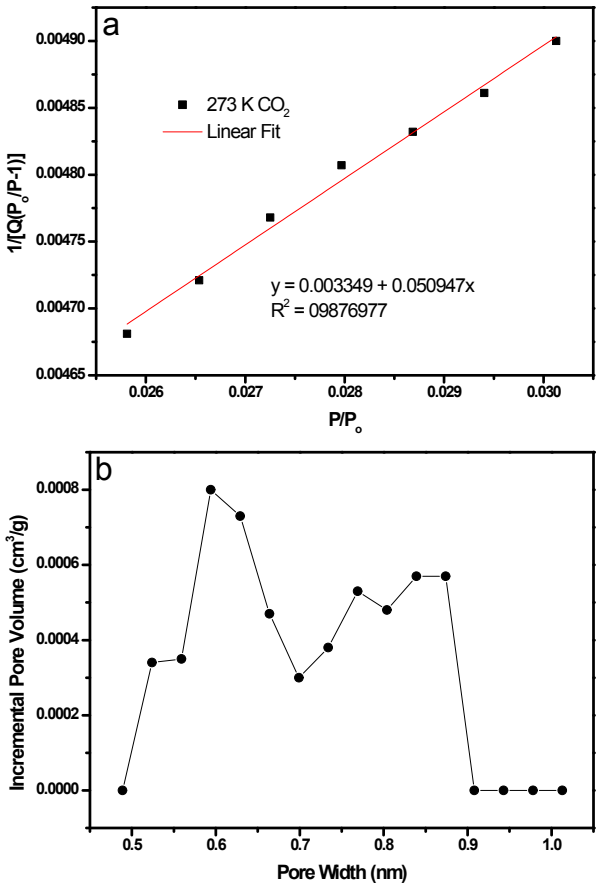

Fig. S2 (a) The BET surface areas of POSS-T_8A obtained from the CO_2 adsorption isotherm at 273 K, S_{BET} = 70.2773 m^2/g. (b) Non-local density functional theory pore size distribution of POSS-T_8A.

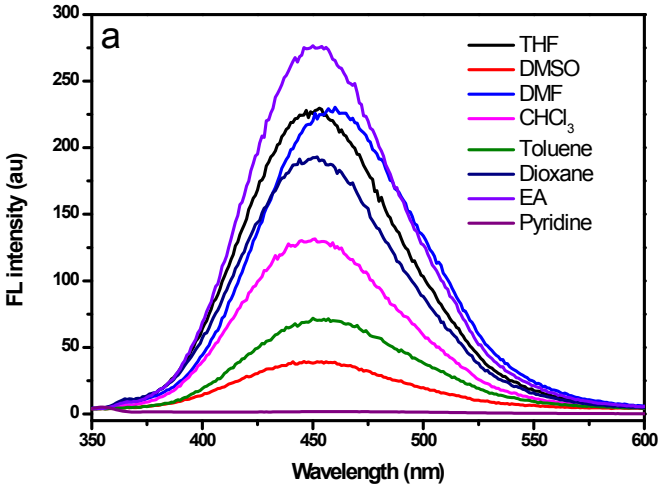

b

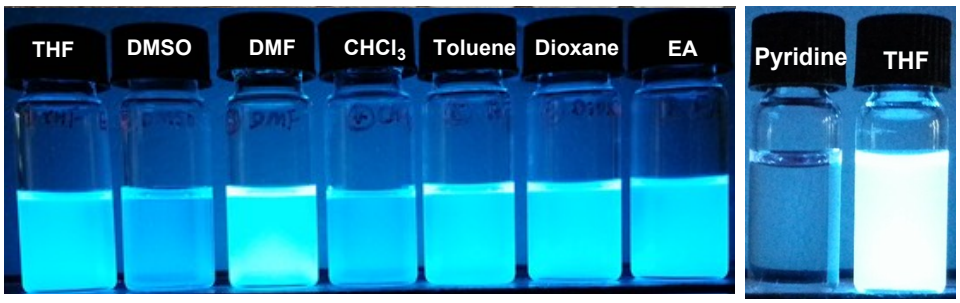

Fig. S3 (a) Fluorescence spectra of POSS-T_8A in different solvents (λ_{ex} = 314 nm, [POSS-T_8A] = 1.0×10^{-5} M. (b) Photographs of POSS-T_8A in different solutions taken under UV illumination (λ_{ex} = 365 nm)).

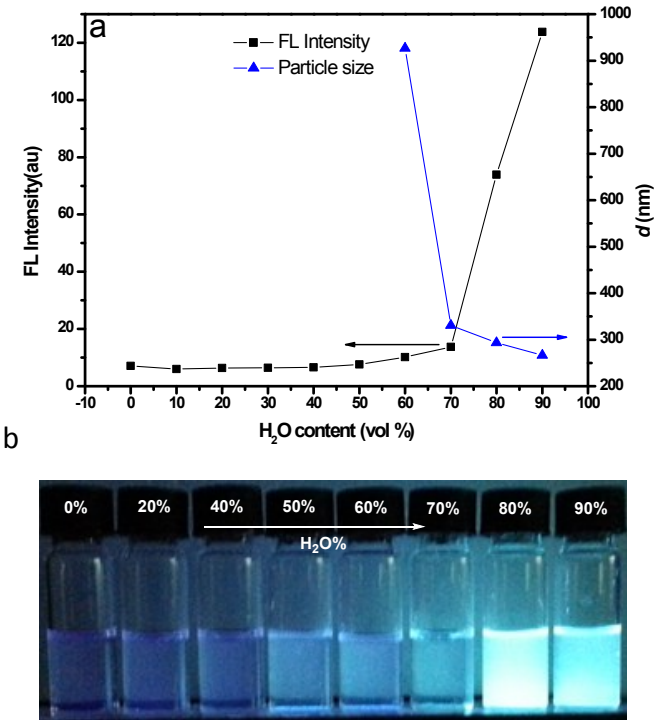

Fig. S4 (a) Fluorescence spectrum and particle size (*d*) and of POSS-T_8B in THF-H_2O mixture. [C] = 1.0 × 10^{-5} M, particle size data measured as a function of absorbance at 633 nm. (b) Photographs of POSS-T_8B in THF/H_2O mixtures taken under UV illumination (λ_{ex} = 365 nm)).

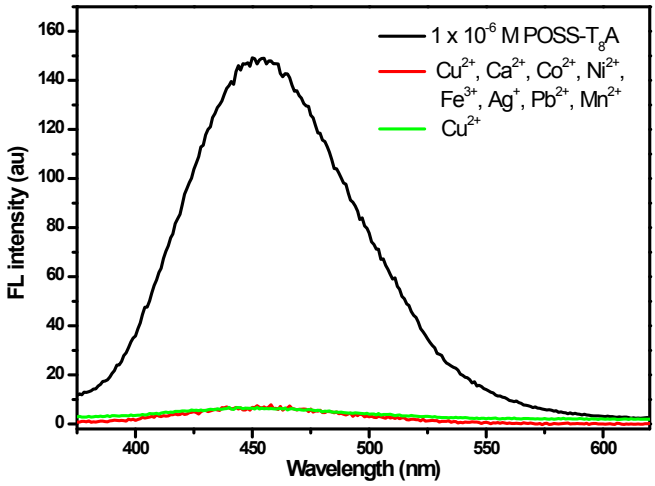

Fig. S5 Fluorescence titration spectra of POSS-T_8A upon addition of $Cu(NO_3)_2$ or with addition of mixed metal ions in DMSO. λ_{ex} = 314 nm, [POSS-T_8A] = 1.0 × 10^{-6} M, [Cu^{2+}] = 1.0 × 10^{-3} M, [ions] = 1.0 × 10^{-3} M.

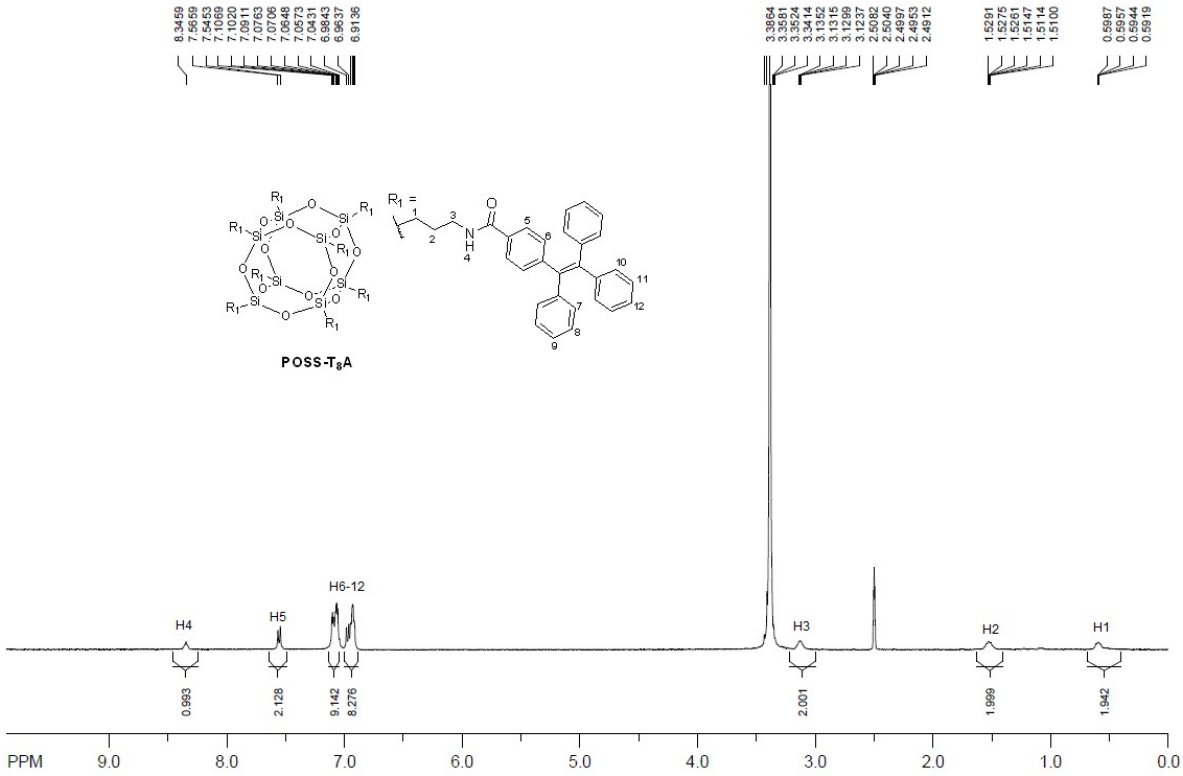

Fig. S6 ^{1}H NMR spectrum of POSS-T_8A in DMSO-d_6.

Table S1. Particle sized and quantum yield of microsized polymer particle of POSS-T_8A in different solvents.

	Solvent	1×10^{-5} M		
		Size (nm)	Count (kcps)	ϕ_f
1	THF	545.8	8.5	0.5293
2	DMSO	291.4	5.6	0.4310
3	DMF	841.8	8.8	0.3841
4	$CHCl_3$	406.2	8.5	0.3291
5	Toluene	1793.1	5.4	0.2272
6	Dioxane	355.1	9.0	0.4508
7	EA	154.7	8.7	0.8312
8	Pyridine	Not detectable	Not detectable	0.0006

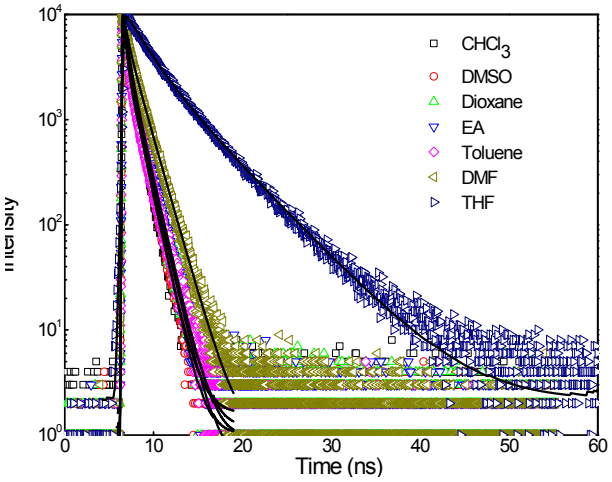

Fig. S7 Fluorescence lifetime of POSS-T_8A in different solvents.

Table S2. List of fitting results obtained from time-resolved fluorescence lifetime decay profiles collected at 465 nm of POSS-T_8A in different solvents.

solvent	τ_1/ns	τ_2/ns	τ_3/ns	<τ>/ns
$CHCl_3$	0.03 (6.42%)	0.56 (42.64%)	1.17 (50.94%)	0.99
DMSO	0.27 (26.60%)	1.08 (74.40%)	--	1.01
Dioxane	0.47 (36.79%)	1.20 (63.21%)	--	1.07
EA	0.50 (34.81%)	1.20 (65.19%)	--	1.07
Toluene	0.30 (35.60%)	1.22 (64.40%)	--	1.11
DMF	0.47 (14.77%)	1.46 (85.23%)	--	1.41
THF	2.09 (34.30%)	5.00 (65.70%)	--	4.47

The time-resolved fluorescence lifetimes of POSS-T_8A in different solvents were measured using a time-correlated single photon counting (TCSPC) spectrofluorimeter (FluoroCube, Horiba Jobin Yvon). The samples were excited at 375 nm using a pulsed diode laser (NanoLED-375L, Horiba Jobin Yvon). The fluorescence decay profiles were analyzed using the Horiba Jobin Yvon Datastation software and the goodness of fit was assessed by considering the reduced chi-square (χ^2) value and the randomness of the weighted residuals. All measurements were performed at ambient conditions. All measurements were performed at ambient conditions.

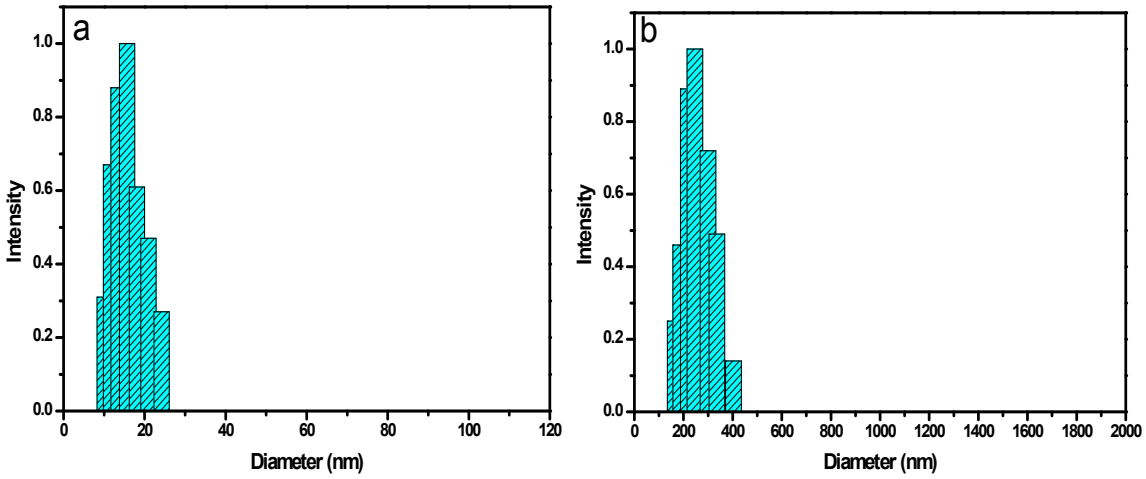

Fig. S8 (a) Particle size distribution of POSS-T_8A·Cu^{2+} in DMSO. (b) Particle size distribution of POSS-T_8A recovered by CN^- in DMSO. [C] = 1.0 × 10^{-5} M, particle size data measured as a function of absorbance at 633 nm.

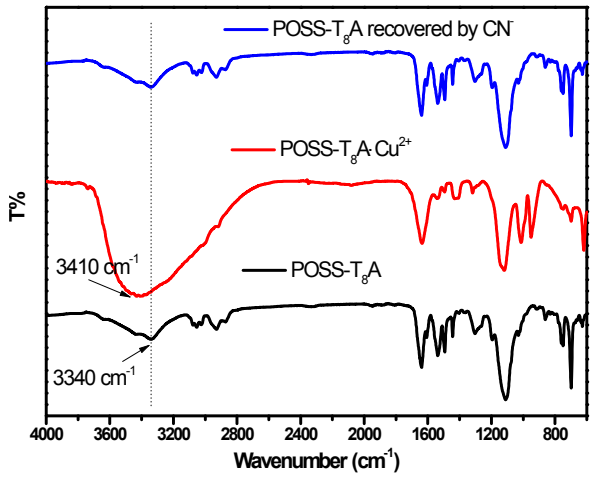

Fig. S9 FTIR spectra of POSS-T_8A, POSS-T_8A·Cu^{2+} and POSS-T_8A recovered by CN^-.

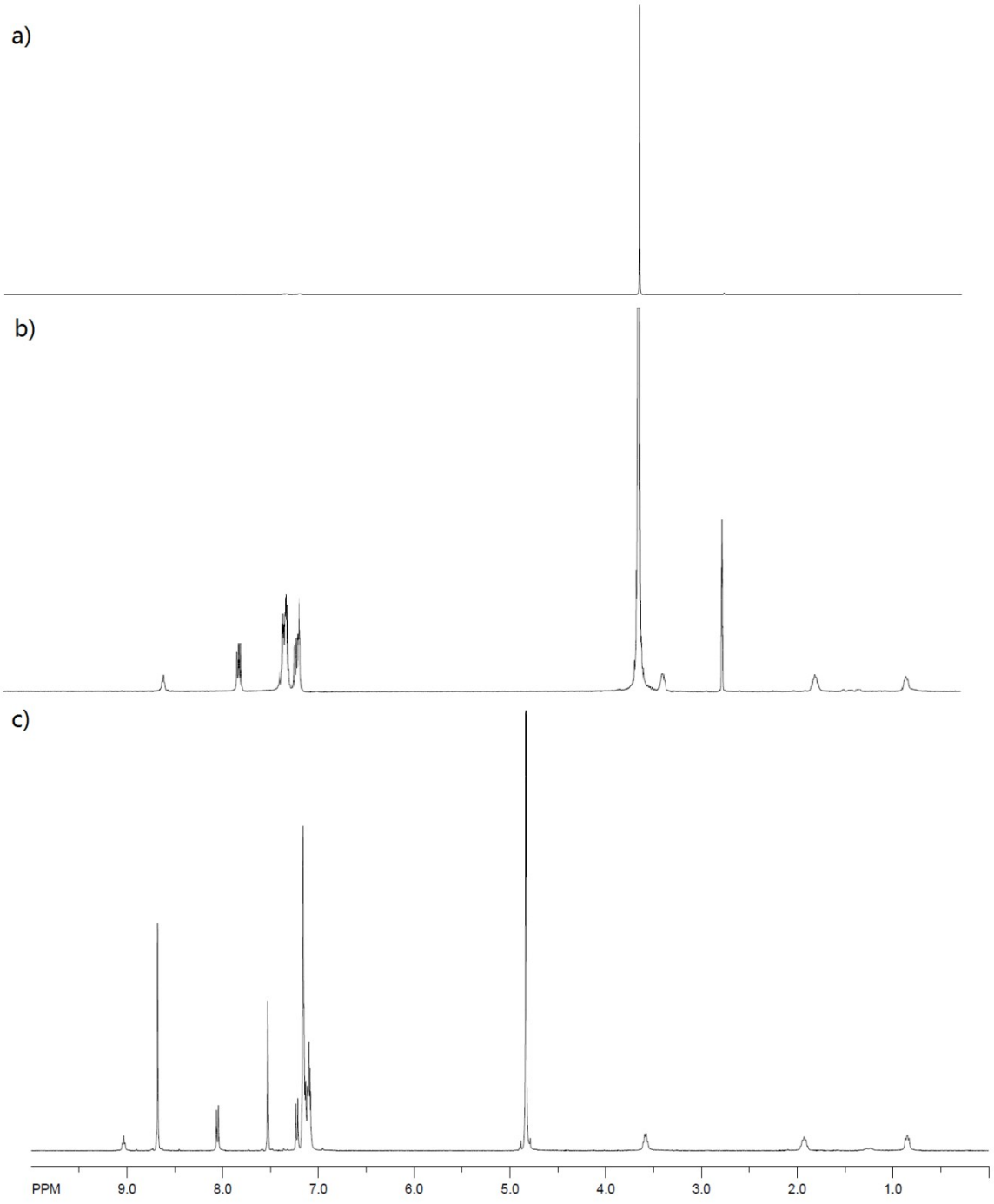

Fig. S10 (a) ^{1}H NMR spectrum of POSS-T_8A in DMSO-d_6 (scan number = 2000). (b) ^{1}H NMR spectrum of POSS-T_8A in DMSO-d_6 (scan number = 28000, intensity is amplified by 100 times). (c) ^{1}H NMR spectrum of POSS-T_8A in pyridine-d_5 (scan number = 2000), [C] = 5.0 mg/mL.

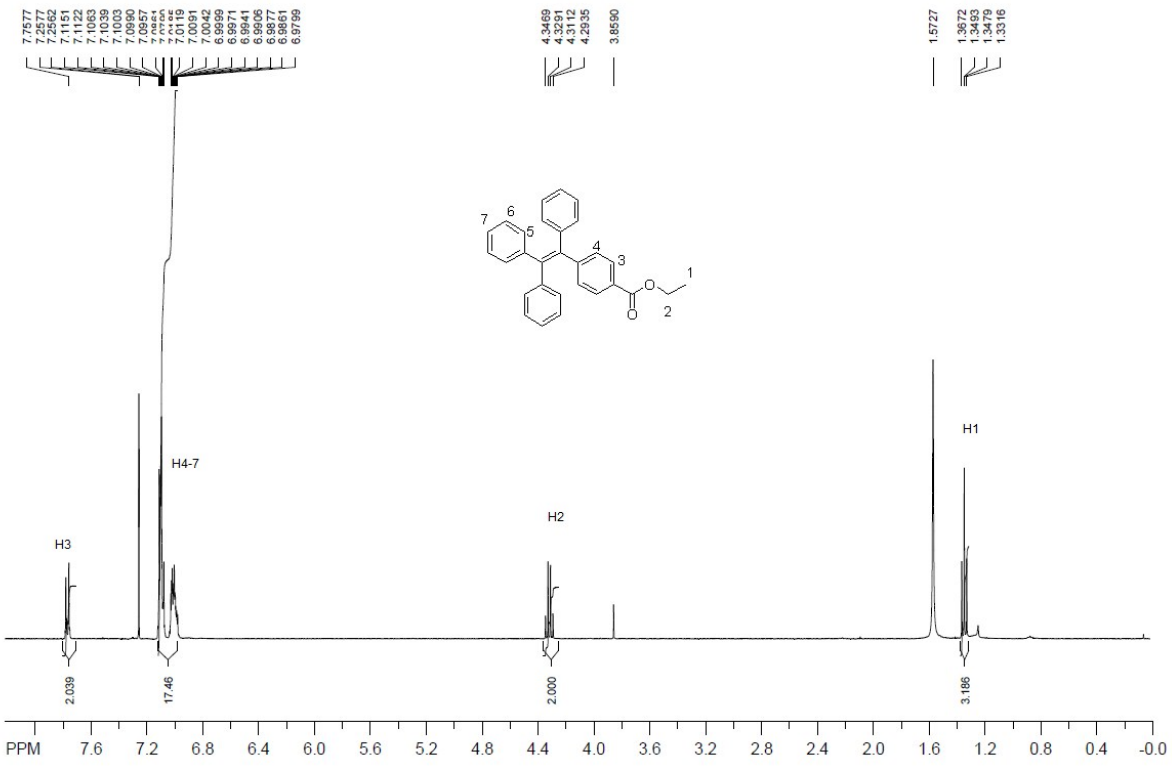

Fig. S11 ^{1}H NMR spectrum of compound **1** in $CDCl_3$.

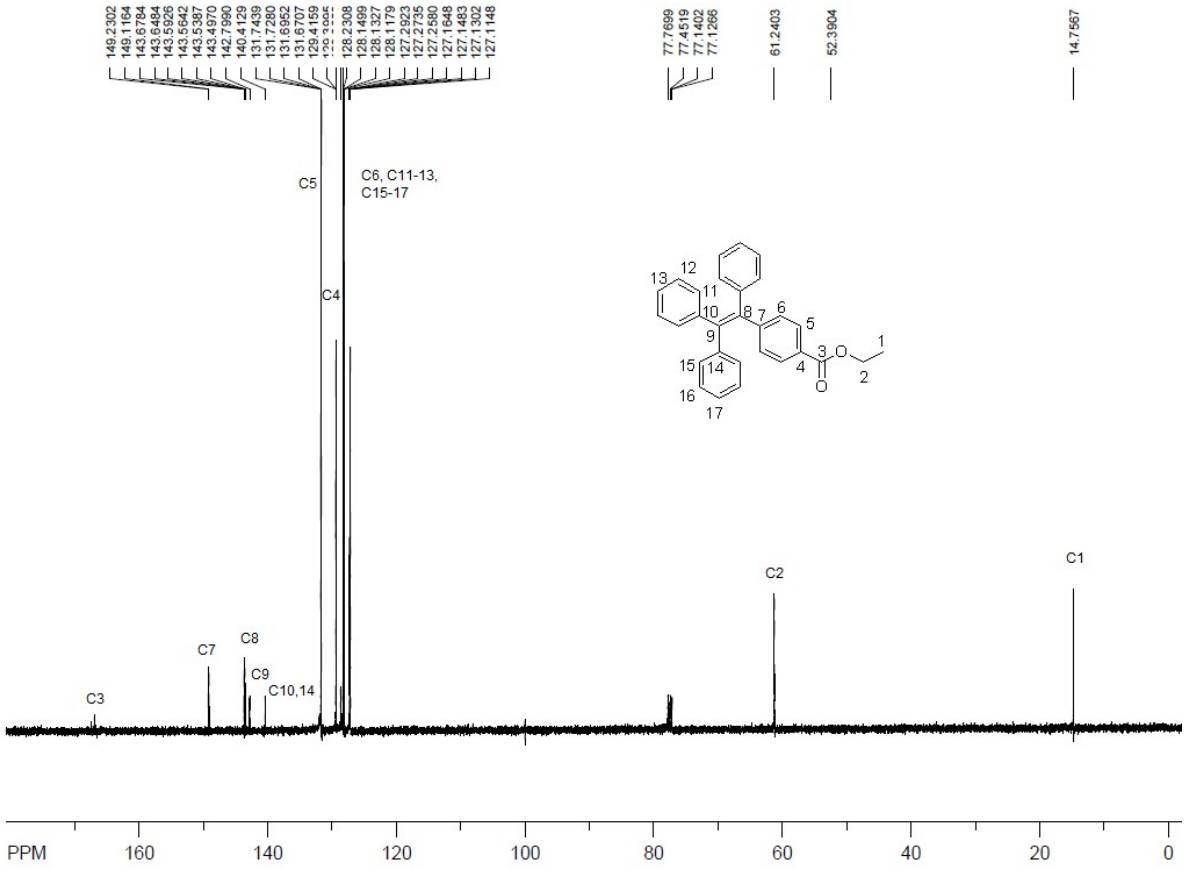

Fig. S12 ^{13}C NMR spectrum of compound **1** in $CDCl_3$.

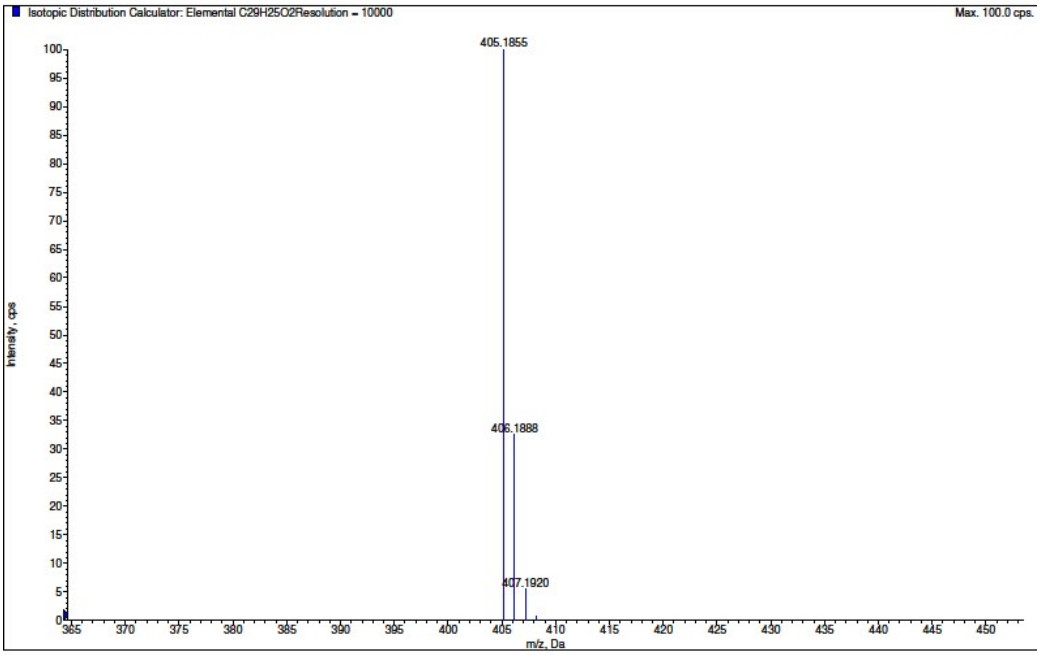

Fig. S13 HRMS spectrum of compound **1**.

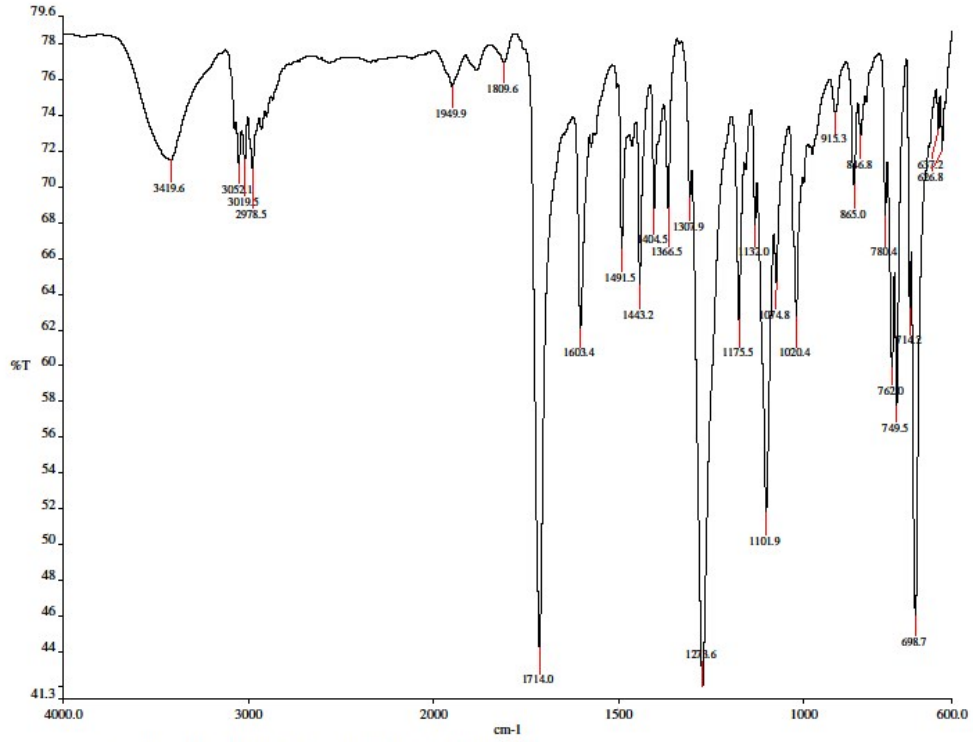

Fig. S14 FTIR spectrum of compound **1** in KBr.

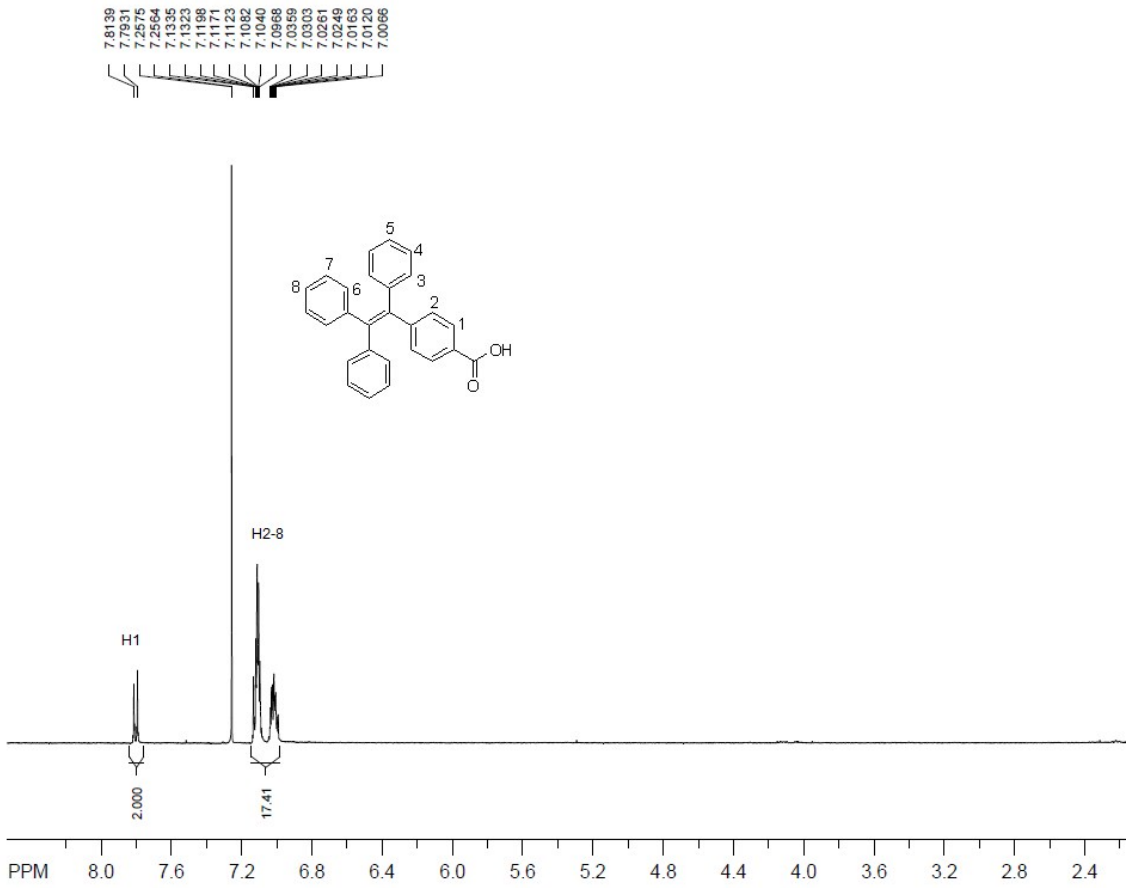

Fig. S15 ^{1}H NMR spectrum of compound **2** in $CDCl_3$.

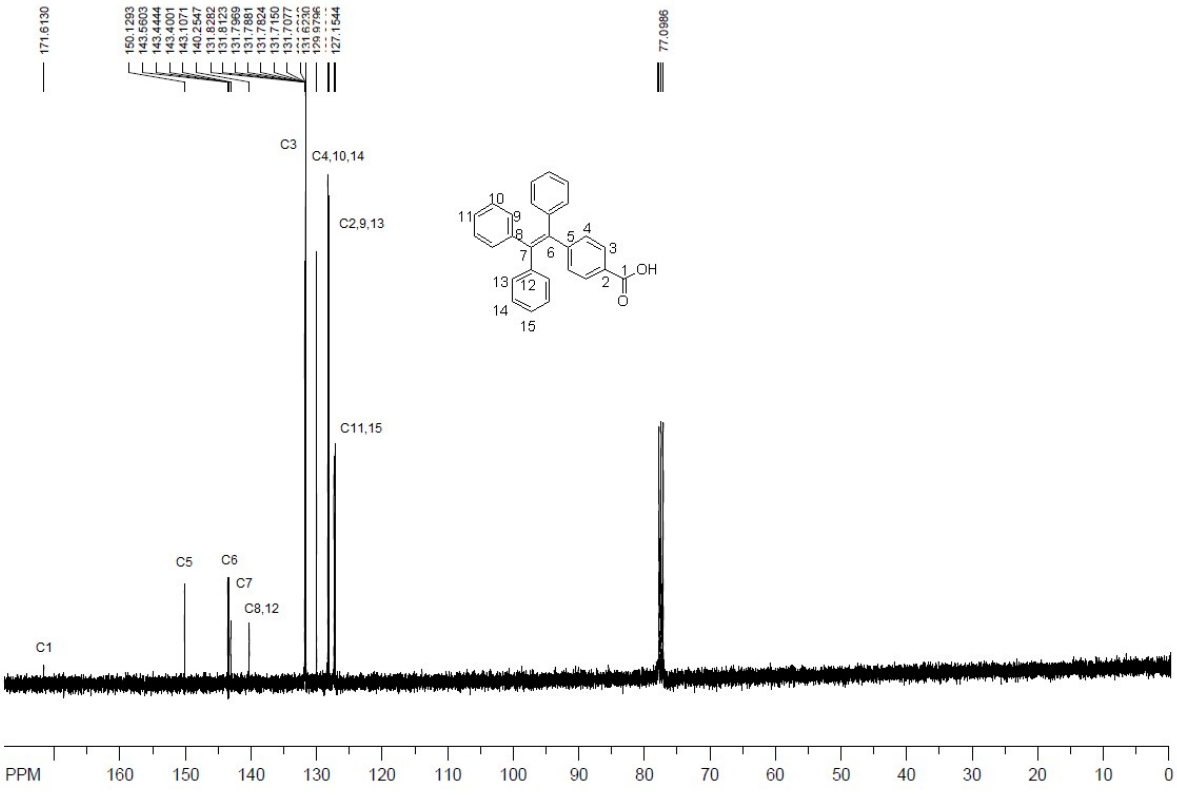

Fig. S16 ^{13}C NMR spectrum of compound **2** in $CDCl_3$.

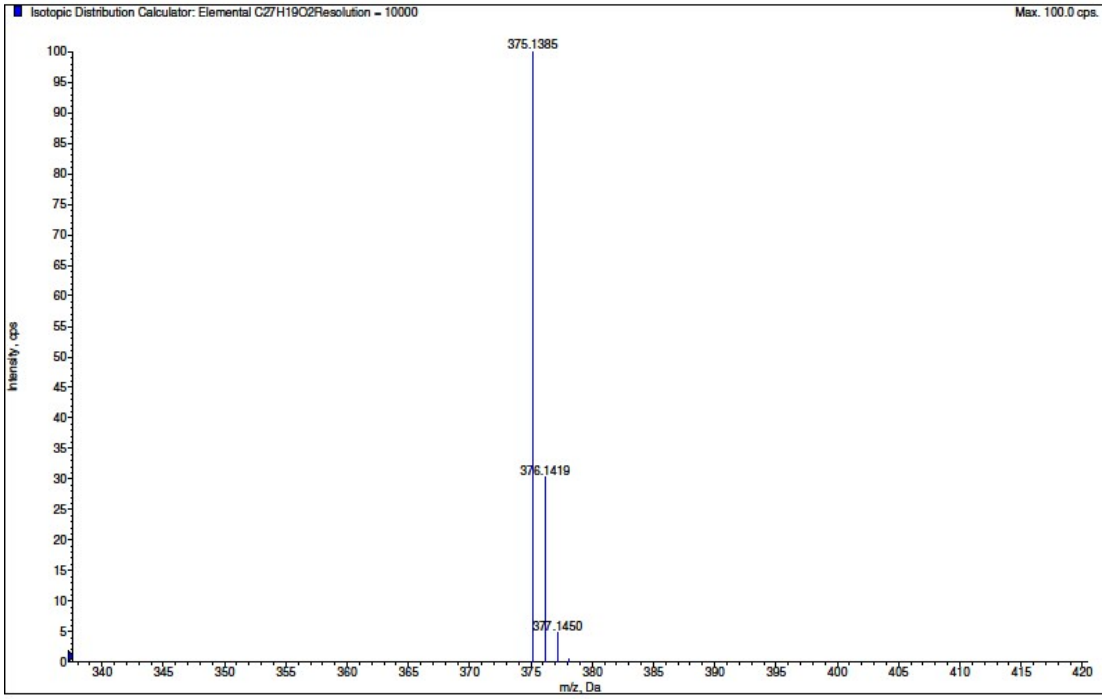

Fig. S17 HRMS spectrum of compound **2**.

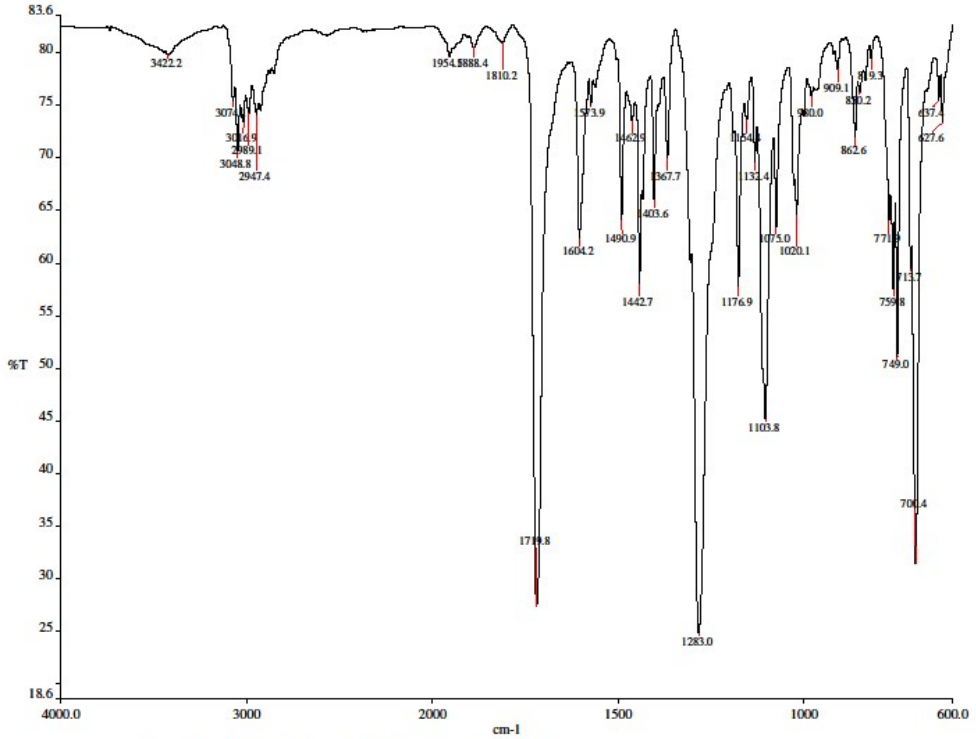

Fig. S18 FTIR spectrum of compound **2** in KBr.

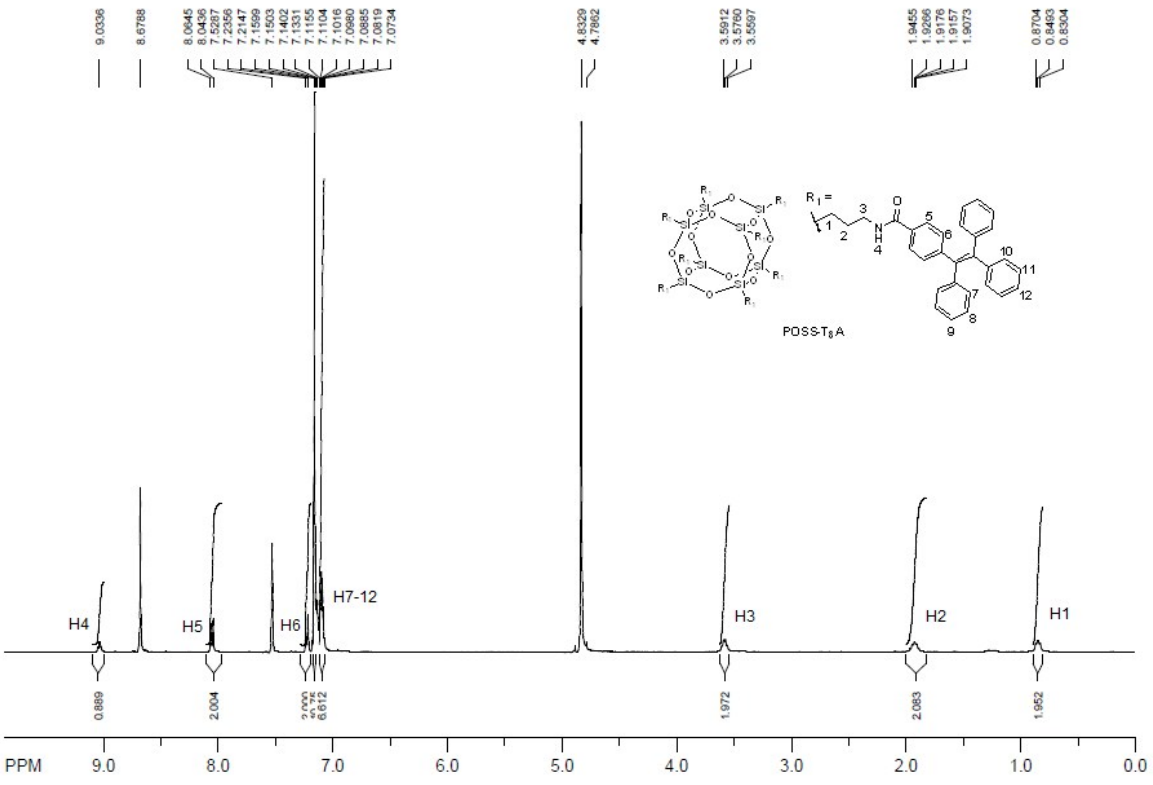

Fig. S19 ^{1}H NMR spectrum of POSS-T_8A in pyridine-d_5.

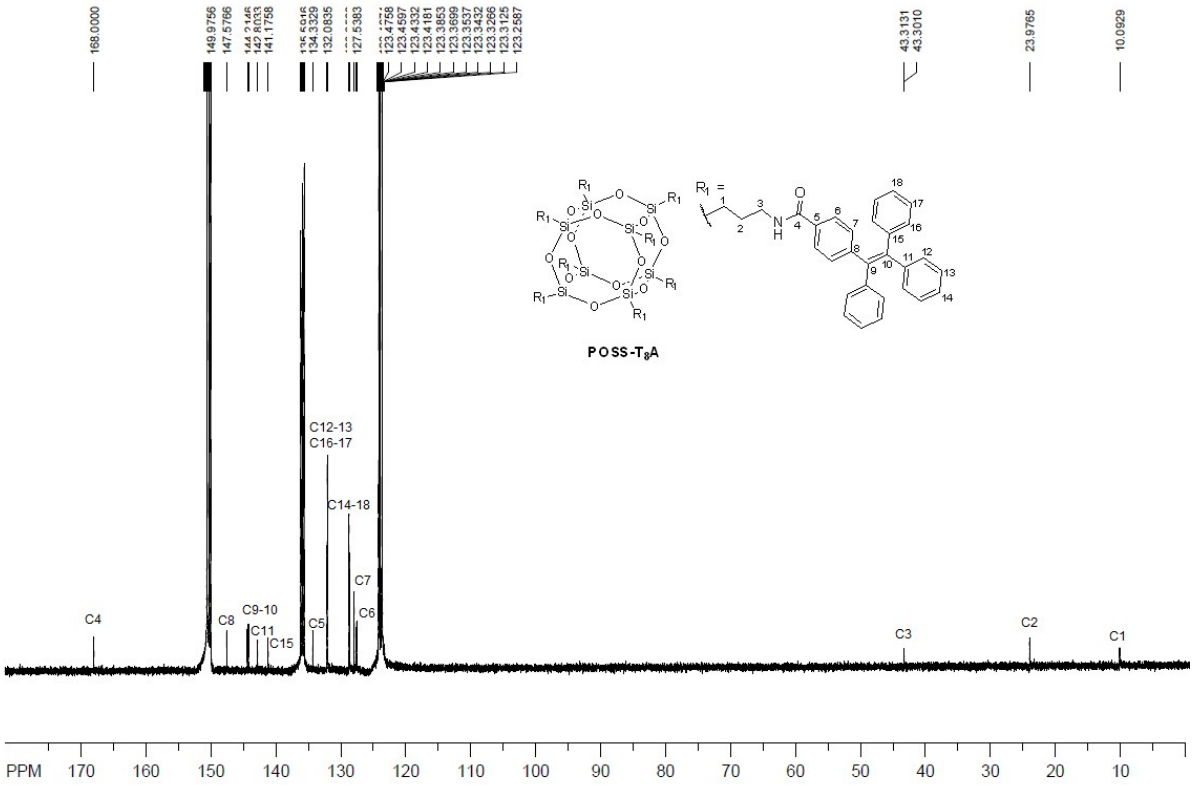

Fig. S20 ^{13}C NMR spectrum of POSS-T_8A in pyridine-d_5.

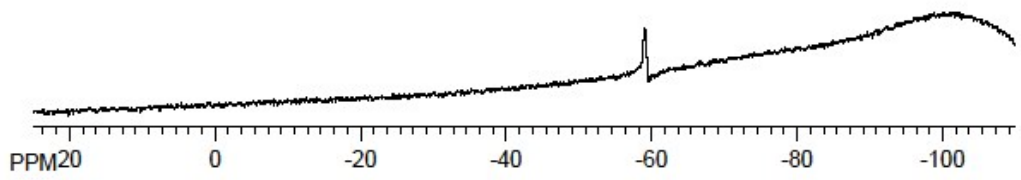

Fig. S21 ^{29}Si NMR spectrum of POSS-T_8A in pyridine-d_5.

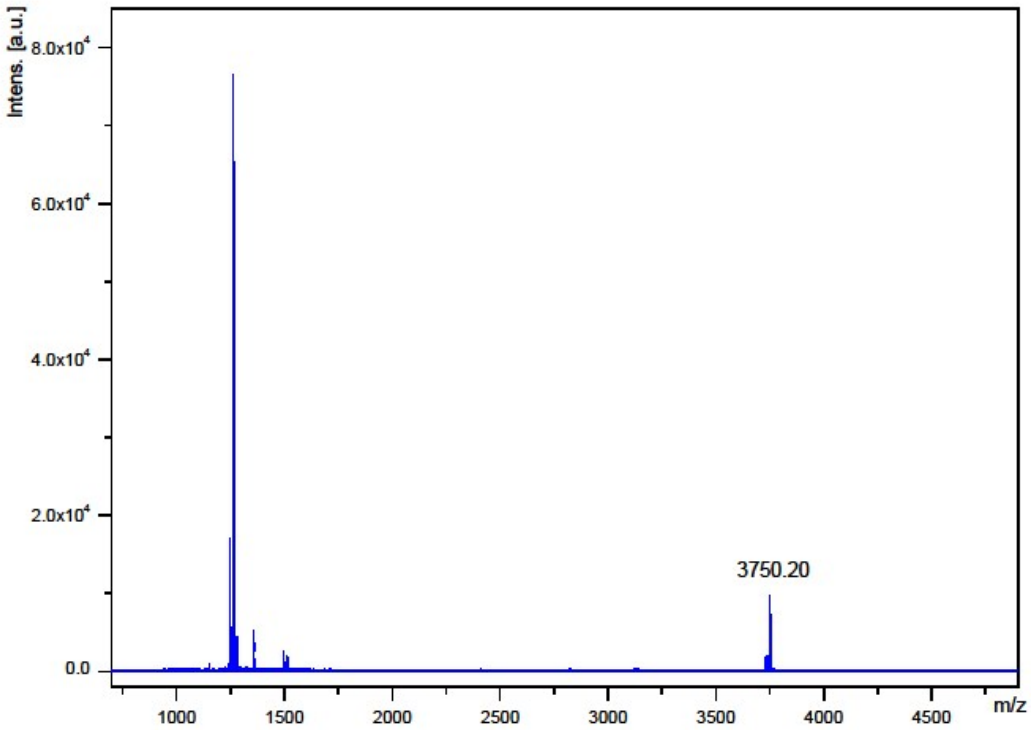

Fig. S22 MALDI-TOF spectrum of POSS-T_8A.

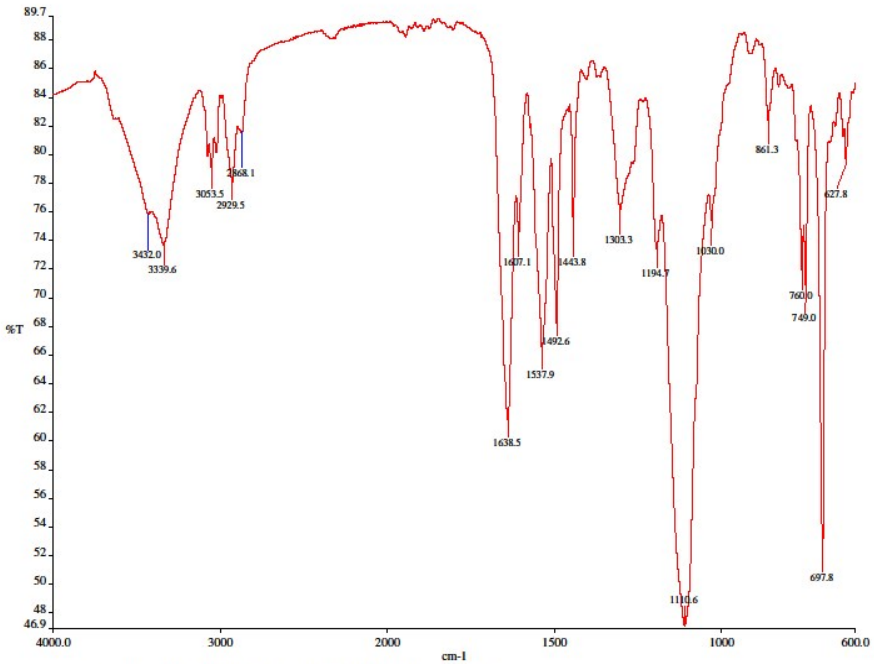

Fig. S23 FTIR spectrum of POSS-T_8A in KBr.

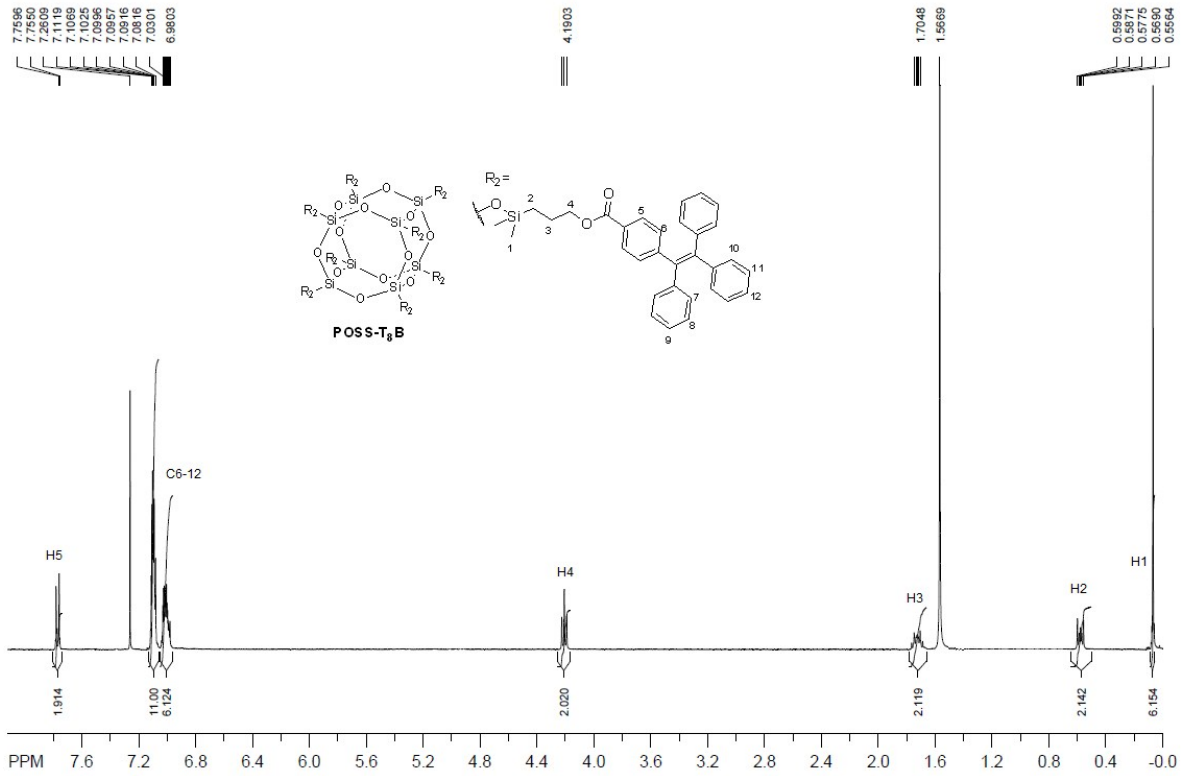

Fig. S24 ^{1}H NMR spectrum of POSS-T_8B in $CDCl_3$.

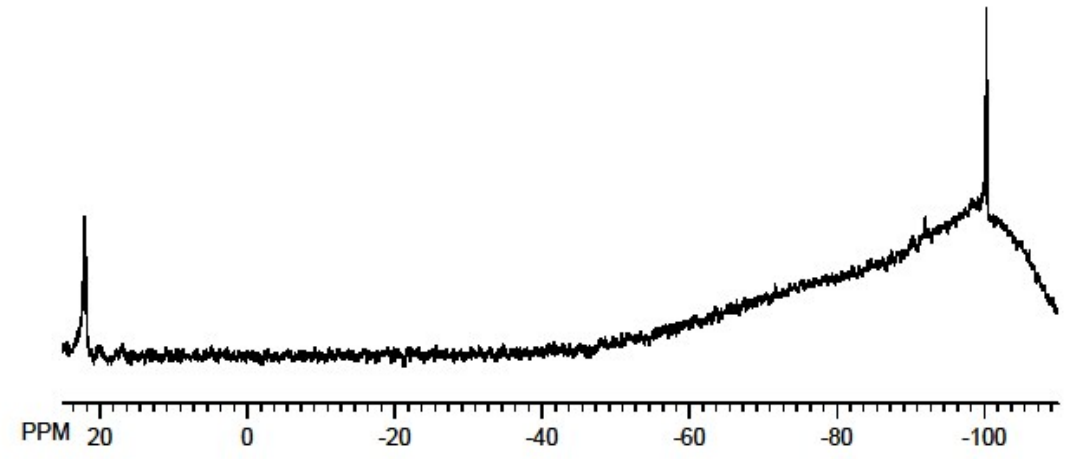

Fig. S25 ^{29}Si NMR spectrum of POSS-T_8B in $CDCl_3$.

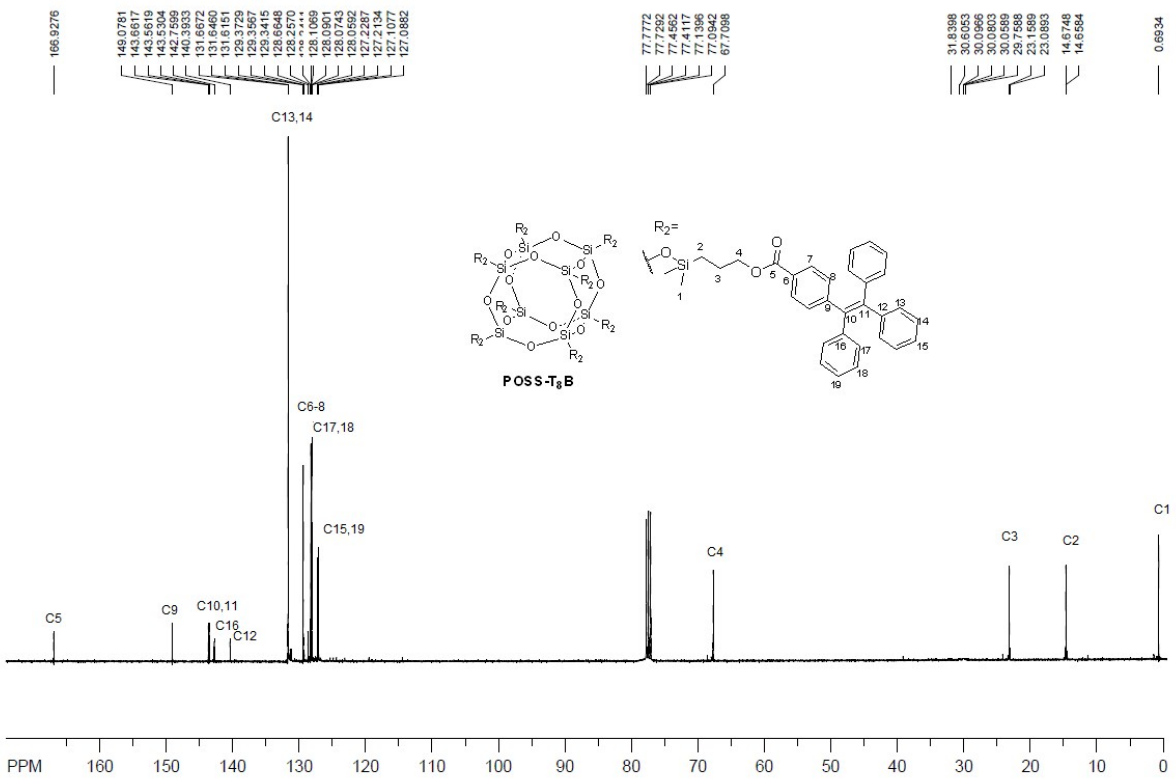

Fig. S26 ^{13}C NMR spectrum of POSS-T_8B in $CDCl_3$.

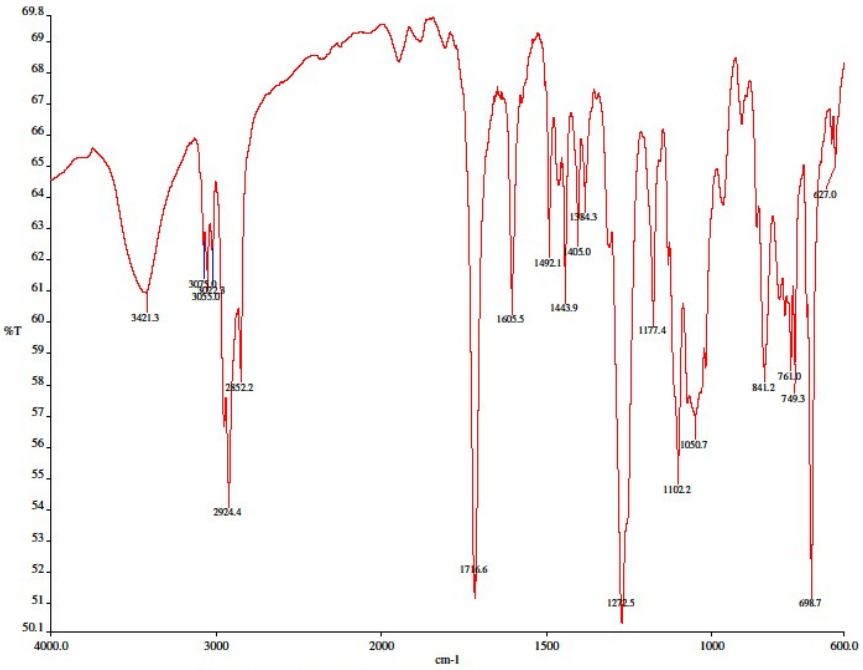

Fig. S27 FTIR spectrum of POSS-T_8B in KBr.

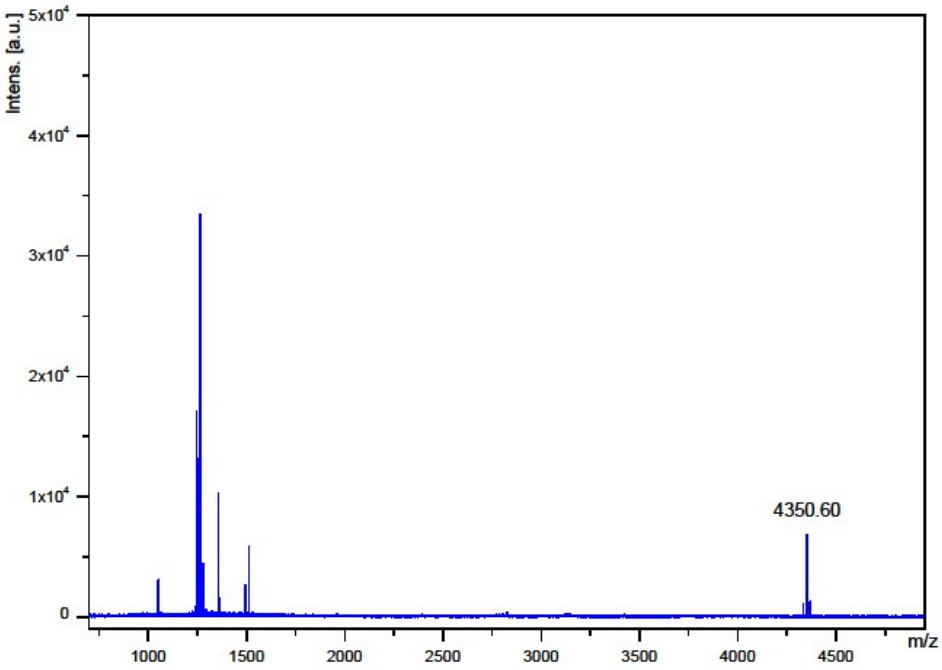

Fig. S28 MALDI-TOF spectrum of POSS-T_8B.

References

1. H. Zhou, F. Liu, X. Wang, H. Yan, J. Song, Q. Ye, B. Z. Tang, J. Xu. *J. Mater. Chem. C,* 2015, **3**, 5490.